Active Fault Tolerant Control of MuPAL-α Using Sliding Modes

L. Chen*, H. Alwi*, C. Edwards* and M. Sato**

Abstract

This paper proposes a simple adaptive sliding mode observer to estimate the effectiveness level of actuators and uses this information as part of an active fault tolerant controller. These observers create an FDI scheme at a 'local' level and the effectiveness estimates are used to drive the online control allocation component in the overall scheme. The approach has been tested on a model of JAXA's MuPAL-α experimental aircraft. The nonlinear simulation results, in fault free and faulty situations, show the efficacy of the scheme. Furthermore, the proposed sliding mode observer has been tested offline using previously collected MuPAL-α flight data and good results are achieved.

I. Introduction

In the last decade, a series of cutting-edge aerospace-based fault detection and isolation (FDI) and fault tolerant control (FTC) projects have been funded by the European Union, such as GARTEUR FM-AG16 [1], ADDSAFE [2], RECONFIGURE [3], [4] and most recently VISION. Thanks to the H2020/Japan co-funded project VISION (Validation of Integrated Safety-enhanced Intelligent flight cONtrol), advanced FDI/FTC approaches developed within the academic community will be verified/validated via piloted flight tests.

Sliding mode control schemes have an inherent capability to reject so-called matched uncertainty i.e. uncertainty which occurs in the channels in which the control signals act [5]. It is easy to recognize that actuator faults and failures, by their very definition, act in these channels and therefore can be considered to be a particular form of matched uncertainty [6]. Consequently, sliding mode controllers can be considered natural candidates for use as fault tolerant controllers. Recent work has demonstrated the theoretical benefits of employing sliding mode controllers within a control allocation framework for over-actuated systems [7], [8]. In these papers, online control allocation is exploited in conjunction with a sliding mode control scheme, and the actuator effectiveness levels are explicitly used as part of the control law in order to mitigate total failures.

In this paper, a simple adaptive sliding mode observer is developed to reconstruct the actuator effectiveness gains. The fault reconstruction signal is created by exploiting the so-called 'equivalent output error injection' signal [5], [9]. If sliding occurs, under the hypothesis of persistent excitation in terms of system inputs, the adaptation process ensures the fault reconstruction signal estimates the actuator effectiveness gains (with exponential convergence to the actual values). By using the adaptive observer proposed in this paper, the actuator effectiveness estimate will not be affected by the singularity problem suffered by previous sliding mode estimation designs in situations in which the system inputs become close to zero.

The control law used here is identical to the one flight tested in [10]. In the preliminary implementation described in [10], knowledge of the actuator effectiveness levels *was assumed to be known perfectly*. The contribution of this paper is to introduce a practical implementable observer scheme to estimate these effectiveness levels based on local actuator information. The observers in this paper will be integrated with the control laws in [10]. The results in this paper therefore represent precursor tests on a nonlinear model prior to future flight testing with MuPAL-α [11], [12]. To prepare for the future flight tests with MuPAL-α, the overall sliding mode online control allocation scheme (including the FDI estimate component) is evaluated on a 6-DOF nonlinear simulation model. The validity of the model has been confirmed by the comparison between flight test results and off-line calculations with the designed controllers in [12]. The nonlinear simulation results presented in this paper show the efficacy of the scheme in both fault free and faulty situations. Furthermore, as a further check, the efficacy of the adaptive sliding mode observer is also evaluated offline (and open loop) using previously collected flight test data from [10].

II. Sliding mode online control allocation

This section briefly describes the overall LPV sliding mode online control allocation scheme.

A. An adaptive LPV sliding mode observer

In this section, a simple adaptive LPV sliding mode observer is developed, at a 'local' actuator system level, to reconstruct the actuator effectiveness levels to identify the presence of faults. This is based on the hypothesis that each critical actuator provides local measurements of the command and resulting actuator position to the FDI scheme. The observer is not computationally heavy. Thus, it can be expected to be implemented on the Fly-By-Wire (FBW) system of MuPAL-α. In many modern aerospace systems the position of the actuators are measured and used locally for safety monitoring in just such an architecture [13].

* College of Engineering, Mathematics and Physical Sciences, University of Exeter, EX4 4QF, UK. lc427@exeter.ac.uk, h.alwi@exeter.ac.uk, C.Edwards@exeter.ac.uk

** Japan Aerospace Exploration Agency, Mitaka, Tokyo 181-0015, Japan. sato.masayuki@jaxa.jp

Consider a single input, signal output (SISO) actuator dynamic subject to a fault modelled as

$$\begin{aligned} \dot{x}_l(t) &= a_l(\rho)x_l(t) + b_l(\rho)w(t)u_l(t-h) \\ y_l(t) &= c_l x_l(t) \end{aligned} \tag{1}$$

with a known time delay ($h > 0$) and $x_l(\tau) = x_l(0)$ for all $\tau \in [-h, 0]$. In (1), the quantities $x_l \in \mathbb{R}$ and $u_l \in \mathbb{R}$ denote the actuator state and the command input respectively. The term $y_l(t) \in \mathbb{R}$ represents the measured position of the actuator. The time varying scheduling parameter $\rho \in \mathbb{R}^{n_r}$ is assumed to be measured perfectly and to belong to a polytope $\Omega \subset \mathbb{R}^{n_r}$. In (1), the scalar function $w(t) \in [0 \quad 1]$ represents the effectiveness levels of the actuator (to be estimated) [6], [14]. If $0 < w(t) < 1$, the actuator behaves with reduced effectiveness (i.e. some level of fault is present). For a fault-free actuator $w(t) = 1$, and for a completely failed actuator $w(t) = 0$. In this paper, the time delay h is assumed to be fixed and known.

Lemma 2.1: [15] A bounded and piecewise continuous vector or matrix $\Theta(t)$ is Persistently Exciting (PE), if for all $t > 0$, there exists $T > 0$ and $\varepsilon > 0$, such that

$$\int_t^{t+T} \Theta(\sigma)^T \Theta(\sigma) d\sigma \geq \varepsilon I \tag{2}$$

Furthermore under these conditions, the system

$$\dot{\xi} = -\Theta(t)^T \Theta(t)\xi \tag{3}$$

is exponentially stable. ■

Assumption 2.1: It is assumed that

i) $a_l(\rho) < 0$ for all $\rho \in \Omega$;
ii) the scalar function $w(t)$ is slow varying, i.e. $\dot{w} \approx 0$;
iii) the term $b_l(\rho)u_l(t-h)$ is PE.

Remark 2.2: Assumption (iii) implies the trajectory, and hence $u_l(t-h)$, must be sufficiently exciting.

The proposed adaptive sliding mode observer is

$$\begin{aligned} \dot{\hat{x}}_l(t) &= a_l(\rho)\hat{x}_l(t) + b_l(\rho)\hat{w}(t)u_l(t-h) - g_l(\rho)e_y(t) - v_l(t) \\ \hat{y}_l(t) &= c_l\hat{x}_l(t) \end{aligned} \tag{4}$$

where $e_y = y_l - \hat{y}_l$ and $v_l = k(t)sign(e_y)$ where $k(t)$ denotes the positive real modulation gain to be selected to ensure sliding. In (4) $\hat{w}(t)$ denotes the estimate of the effectiveness level and $g_l(\rho)$ is a gain to be selected.
Define $e_l = x_l - \hat{x}_l$ and $\tilde{w} = w - \hat{w}$, then the following error system is obtained from (1) and (4):

$$\dot{e}_l = (a_l(\rho) + g_l(\rho)c_l)e_l + b_l(\rho)u_l(t-h)\tilde{w} + v_l \tag{5}$$

Since $(a_l(\rho), c_l)$ are scalars, there always exists a $g_l(\rho)$ such that $(a_l(\rho) + g_l(\rho)c) < 0$.

Proposition 2.1: If the modulation gain $k(t)$ is chosen as

$$k(t) = |b_l(\rho)||u_l(t-h)|(|\hat{w}(t)| + 1) + \eta \tag{6}$$

where $\eta > 0$, then e_y will converge to zero and a sliding motion will take place in finite time.

Proof: Let $\tilde{a}(\rho) = a_l(\rho) + g_l(\rho)c_l$ and define as a candidate Lyapunov function $V = \frac{1}{2}e_y^2$. Then it follows

$$\dot{V} = e_l^2 c_l^2 \tilde{a}(\rho) + e_l c_l^2 (b_l(\rho)u_l(t-h)\tilde{w} + v_l) \leq e_l c_l^2 (b_l(\rho)u_l(t-h)\tilde{w} + v_l) \tag{7}$$

since $\tilde{a}(\rho) < 0$. Using the fact $|\tilde{w}| \leq 1 + |\hat{w}|$

$$\dot{V} \leq |e_l c_l^2|(|b_l(\rho)||u_l(t-h)|(1 + |\hat{w}|) - k(t)) \tag{8}$$

If (6) is satisfied, $\dot{V} \leq -\eta|c_l||e_y| \leq -\eta|c_l|\sqrt{2V}$ and e_y will converge to zero and a sliding motion will take place in finite time. ■

During the sliding motion, $\dot{e}_l(t) = e_l(t) = 0$. Substituting these quantities into (4) yields

$$v_{leq} = -b_l(\rho)u_l(t-h)\tilde{w} \tag{9}$$

where v_{leq} is the equivalent output error injection signal in (5) necessary to maintain sliding [5].
To create $\hat{w}$, the following adaptation algorithm is proposed:

$$\dot{\hat{w}} = -\tau b_l(\rho)u_l(t-h)v_{leq} \quad \text{and} \quad \hat{w}(0) = 1 \tag{10}$$

where $\tau > 0$ is a design scalar. Using the assumption $\dot{w} \approx 0$, $\dot{\tilde{w}} \approx -\dot{\hat{w}}$ and substituting (9) into (10) it follows

$$\dot{\tilde{w}} = -\tau(b_l(\rho)u_l(t-h))^2\tilde{w} \tag{11}$$

Using the assumption that $b_l(\rho)u_l(t-h)$ is PE, from Lemma 2.1, the system in (11) is exponentially stable. As a consequence, $\tilde{w} \to 0$ and $\hat{w} \to w$ as $t \to \infty$, and the effectiveness level of the actuator can be estimated in a 'local' level.

Remark 2.3: Without using the adaptive component in (10), the term $wu_l(t-h)$ will be reconstructed (instead of w). In this situation, if $u_l(t-h)$ is close to zero, it is difficult to calculate a fault reconstruction signal from $wu_l(t-h)$.

B. Sliding mode online control allocation

Suppose the LPV representation of the *overall plant*, subject to actuator faults/failures and 'matched' disturbances is

$$\begin{aligned}\dot{x}_p(t)&=A_p(\rho)x_p(t)+B_p(\rho)W(t)u_p(t)+D_p(\rho)\xi(t)\\ y_c(t)&=C_c x_p(t)\end{aligned} \tag{12}$$

where $A_p(\rho) \in \mathbb{R}^{n\times n}$, $B_p(\rho) \in \mathbb{R}^{n\times m}$, $C_c \in \mathbb{R}^{l\times n}$ and $l < m$. Here it is assumed there are $l < m$ controlled outputs and therefore redundancy exists in the system. The state vector and the control input are denoted by $x_p \in \mathbb{R}^n$ and $u_p \in \mathbb{R}^m$, respectively. In (12), $D_p(\rho) \in \mathbb{R}^{n\times k}$ represents the disturbance distribution matrix and $\xi(t) \in \mathbb{R}^k$ denotes a 'matched' disturbance which is bounded and assumed to satisfy $\|\xi(t)\| \leq \alpha(t, x)$. In (12), the weighting function matrix $W(t) := \mathrm{diag}(w_1(t), \ldots, w_m(t))$ where the time varying scalar functions $w_1(t), w_2(t), \ldots w_m(t)$ represent the effectiveness levels of the actuators which tie in with the actuator models described in (1). In this paper, it will be assumed each scalar $w_i(t)$ is independently reconstructed, using a collection of the adaptive sliding mode observers as proposed in Section II-A. Note the system measurements in (12) do not (generally) include the local measurements used in (1).
As in [9], define integrator states to induce tracking performance according to

$$\dot{x}_r = r(t) - C_c x_p(t) \tag{13}$$

where $r(t)$ is a differentiable command signal. Combining (12) and (13) yields an augmented state space system of the form

$$\underbrace{\begin{bmatrix}x_r(t)\\ x_p(t)\end{bmatrix}}_{x_a(t)} = \underbrace{\begin{bmatrix}0 & -C_c\\ 0 & A_p(\rho)\end{bmatrix}}_{A_a(\rho)}\begin{bmatrix}x_r(t)\\ x_p(t)\end{bmatrix} + \underbrace{\begin{bmatrix}0\\ B_p(\rho)\end{bmatrix}}_{B_a(\rho)} W(t)u_p(t) + \underbrace{\begin{bmatrix}I_l\\ 0\end{bmatrix}}_{B_c} r(t) + \underbrace{\begin{bmatrix}0\\ D_p(\rho)\end{bmatrix}}_{D_a(\rho)} \xi(t) \tag{14}$$

As in [10], suppose $B_a(\rho)$ in (14) can be factorized as

$$B_a(\rho) = B_v B_2(\rho) \tag{15}$$

where $B_v \in \mathbb{R}^{(n+l)\times l}$ is a known fixed matrix in which $\mathrm{rank}(B_v) = l$, whilst $B_2(\rho) \in \mathbb{R}^{l\times m}$ is a matrix with varying elements which satisfies $\mathrm{rank}(B_2(\rho)) = l$ for all $\rho \in \Omega$. Since B_v is full column rank, there always exists a coordinate transformation matrix $T_a = \mathrm{diag}(I_l, T_n)$ where $T_n \in \mathbb{R}^{n\times n}$ and $\det(T_n) \neq 0$ such that

$$T_a B_v = \begin{bmatrix}0\\ I_l\end{bmatrix} \tag{16}$$

In the new coordinate system $x(t) = T_a x_a(t)$ it follows

$$\dot{x}(t)=A(\rho)x(t)+\begin{bmatrix}0\\ B_2(\rho)\end{bmatrix} W(t)u_p(t)+B_c r(t)+D(\rho)\xi(t) \tag{17}$$

where $A(\rho) = T_a A_a(\rho) T_a^{-1}$ and $D(\rho) = T_a D_a(\rho)$. As in [10], define a virtual control signal $v(t) \in \mathbb{R}^l$ as

$$v(t) := B_2(\rho)u_p(t) \tag{18}$$

As argued in [10], if the actual physical control signals sent to the actuators are given by

$$u_p(t) := B_2(\rho)^\dagger v(t) \tag{19}$$

where

$$B_2(\rho)^\dagger := \Lambda(t)B_2(\rho)^T(B_2(\rho)\Lambda(t)^2 B_2(\rho)^T)^{-1} \tag{20}$$

and $\Lambda(t) = \mathrm{diag}(\lambda_1(t), \ldots, \lambda_m(t))$ is a weighting matrix chosen to guarantee $\det(B_2(\rho)\Lambda(t)^2 B_2(\rho)^T) \neq 0$, then it is clear that this choice of $B_2(\rho)^\dagger$ in (20) ensures equation (19) is satisfied. In the case when $\Lambda(t) = I$, $B_2(\rho)^\dagger$ is a right pseudo-inverse of $B_2(\rho)$. In this paper, for the purpose of developing an online control allocation scheme, it is assumed $\Lambda(t)$ is the online estimate of $W(t)$ i.e. $\Lambda(t) = \widehat{W}(t)$ where $\widehat{W}(t) = \mathrm{diag}(\hat{w}_1(t), \ldots, \hat{w}_m(t))$ and the $\hat{w}_i(t)$ are estimated from the adaption scheme in Section II-A. Typically $\widehat{W}(t) \neq W(t)$ for all time but assume

$$\Lambda(t) = \widehat{W}(t) = (I + \Delta(t))^{-1} W(t) \tag{21}$$

where $\Delta(t)$ is an unknown diagonal matrix such that

$$\|\Delta(t)\| < \bar{\Delta} < 1 \tag{22}$$

where $\bar{\Delta}$ is a fixed scalar which will be discussed in the sequel. In equation (21), $\Delta(t)$ encapsulates the error in the estimate of $W(t)$.
Define

$$\mathcal{W} \subseteq \{\Lambda(t) = \mathrm{diag}(\lambda_1, \ldots, \lambda_m) : 0 \leq \lambda_i \leq 1\} \tag{23}$$

and assume for all $W(t) \in \mathcal{W}$ and $\rho \in \Omega$,

$$\det(B_2(\rho)\Lambda(t)^2 B_2(\rho)^T) \neq 0 \tag{24}$$

Clearly $\mathcal{W}$ is a nonempty set since $\Lambda(t) = I \in \mathcal{W}$. From (21), in the situation when $\Delta(t) = 0$ and $\Lambda(t) = W(t)$, substituting (19) and (20) into (17) yields

$$\dot{x}(t) = A(\rho)x(t) + \begin{bmatrix} 0 \\ I_l \end{bmatrix} v(t) + B_c r(t) + D(\rho)\xi(t) \tag{25}$$

The aim is to create a virtual control law $v(t)$ to ensure closed-loop stability of the system in (25) for all combinations of faults/failures.

Partition the states in (25) as $x = \mathrm{col}(x_1, x_2)$ where $x_1 \in \mathbb{R}^n$ and $x_2 \in \mathbb{R}^l$. Equation (25) in partitioned form becomes

$$\begin{bmatrix} \dot{x}_1(t) \\ \dot{x}_2(t) \end{bmatrix} = \begin{bmatrix} A_{11}(\rho) & A_{12}(\rho) \\ A_{21}(\rho) & A_{22}(\rho) \end{bmatrix} \begin{bmatrix} x_1(t) \\ x_2(t) \end{bmatrix} + \begin{bmatrix} 0 \\ I_l \end{bmatrix} v(t) + \begin{bmatrix} B_{c1} \\ B_{c2} \end{bmatrix} r(t) + \underbrace{\begin{bmatrix} D_1(\rho) \\ D_2(\rho) \end{bmatrix}}_{D(\rho)} \xi(t) \tag{26}$$

Since $\xi(t)$ is assumed to be 'matched' uncertainty, in (26) $D_1(\rho) = 0$ so that $\mathrm{range}(D(\rho)) \subseteq \mathrm{range}(B_v)$.

C. Define of the switching function

Here $v(t)$ will be designed based on sliding mode concepts as described in [10]. Define a parameter-dependent switching function as

$$s(t) = S(\rho)x(t) \tag{27}$$

where

$$S(\rho) = \begin{bmatrix} M(\rho) & I_l \end{bmatrix} \tag{28}$$

In (28), $M(\rho) \in \mathbb{R}^{l \times n}$ represents the design freedom. Assume that

$$\begin{aligned} A(\rho) &= A_0 + A_1\rho_1(t) \ldots + A_{n_r}\rho_{n_r}(t) \\ M(\rho) &= M_0 + M_1\rho_1(t) \ldots + M_{n_r}\rho_{n_r}(t) \end{aligned} \tag{29}$$

During sliding $s(t) = 0$ and therefore from (27) and (28)

$$x_2(t) = -M(\rho)x_1(t) \tag{30}$$

Substituting (30) into (26) yields the expression for the reduce order sliding motion as

$$\dot{x}_1(t) = \hat{A}_{11}(\rho)x_1(t) + \hat{B}_{c1}r(t) \tag{31}$$

where $\hat{A}_{11}(\rho) = A_{11}(\rho) - A_{12}(\rho)M(\rho)$ and the fixed matrix $\hat{B}_{c1} = B_{c1}$. Since $\hat{A}_{11}(\rho)$ is dependent on $M(\rho)$, the choice of $M(\rho)$ can be viewed as a parameter-dependent state feedback problem for the pair $(A_{11}(\rho), A_{12}(\rho))$. Since the scheduling parameter ρ varies inside a polytope, the parameter-dependent state feedback problem can be solved using the vertex property. As in [16], [10], $M(\rho)$ can be calculated via LPV regional pole placement.

D. Control law with online control allocation

This section considers the development of a virtual control law $v(t)$ to induce and maintain sliding in the most general case where $\Lambda(t)$ is an estimate of $W(t)$, and specifically where $\Lambda(t) = (I + \Delta(t))^{-1}W(t)$ as in (21). Let

$$\mathcal{W}_e = \{\Lambda = \mathrm{diag}(\lambda_1, \ldots, \lambda_m) : B_2(\rho)\Lambda^2 B_2(\rho)^T > \epsilon I_l\} \tag{32}$$

where $\epsilon > 0$ and $0 \leq \lambda_i \leq 1$ and $\rho \in \Omega$. Clearly $\mathcal{W}_e \subset \mathcal{W}$.

Here the virtual control law is selected to contain two components: $v(t) = v_0(t) + v_n(t)$ where

$$v_0(t) = -S(\rho)(A(\rho)x(t) + B_c r(t)) - (M(\dot{\rho}) - M_0)x_1(t) + \Phi s(t) \tag{33}$$

and Φ is a Hurwitz matrix. The nonlinear term

$$v_n(t) = -\mathcal{K}(t,x)\frac{P_2 s(t)}{\|P_2 s(t)\|} \quad \text{if} \quad s(t) \neq 0 \tag{34}$$

where the symmetric positive definite matrix P_2 satisfies

$$P_2\Phi + \Phi^T P_2 = -I_l \tag{35}$$

It is assumed that the uncertainty bound $\bar{\Delta}$ from (22) satisfies

$$\bar{\Delta} < \frac{1 - \Delta_{max}}{\|B_2(\rho)\|\|B_2(\rho)^\dagger\|} \tag{36}$$

for all $\Lambda(t) \in \mathcal{W}_e$ and $\rho \in \Omega$ where the design parameter $0 < \Delta_{max} < 1$. Then the following theorem can be proved.

Theorem 2.1: If the design matrix $M(\rho)$ has been chosen such that $\hat{A}_{11}(\rho)$ is quadratically stable and $\Delta(t)$, capturing the error in estimating $W(t)$, satisfies (36), then choosing

$$\mathcal{K}(t,x) \geq \frac{\|D_2(\rho)\|\alpha(t,x) + \eta_c + (1-\Delta_{max})\|v_0\|}{\Delta_{max}} \tag{37}$$

where the variable η_c is a positive design scalar ensures a sliding motion takes place on $s(t) = 0$ in finite time.

Proof: Please refer to [10]. ■

Remark 2.5: Notice that when $\Lambda = I$, $B_2(\rho)B_2(\rho)^\dagger = I_l$ which implies $\|B_2(\rho)\|\|B_2(\rho)^\dagger\| > 1$ and therefore the right hand side of (36) is always less than unity.

By direct computation, from the definition of $B_2(\rho)^\dagger$ in (20)

$$\|B_2(\rho)^\dagger\|^2 = \lambda_{max}((B_2(\rho)^\dagger)^T B_2(\rho)^\dagger) = \lambda_{max}(B_2(\rho)\Lambda^2 B_2(\rho)^T)^{-1} \tag{38}$$

Therefore if

$$B_2(\rho)\Lambda^2 B_2(\rho)^T > \epsilon I \tag{39}$$

for all $\rho \in \Omega$ then

$$\|B_2(\rho)^\dagger\| < \frac{1}{\sqrt{\epsilon}} \tag{40}$$

and consequently for any $\Lambda(t) \in \mathcal{W}_e$, $\|B_2(\rho)^\dagger\| < \frac{1}{\sqrt{\epsilon}}$.

Thus for a given level of accuracy of effectiveness level estimation $\bar{\Delta}$, using (36), the design parameter Δ_{max} must be chosen to ensure

$$\Delta_{max} < 1 - \frac{\bar{\Delta}\|B_2(\rho)\|}{\sqrt{\epsilon}} \tag{41}$$

Remark 2.6: Note that inequality (41) links together the design of the controller and the performance of the estimator scheme through the choice of the parameter Δ_{max}.

III. Evaluation using the nonlinear MuPAL-α model

In this section, the proposed scheme will be evaluated on a nonlinear simulation model of the JAXA Multi-Purpose Aviation Laboratory (MuPAL-α) research aircraft. This aircraft is based on the 2-propeller engine Dornier Do228-202 aircraft modified to include a research FBW system [11], [12]. The simulation is a nonlinear 6-DOF model whose fidelity has been confirmed in [12]. The nonlinear simulation model contains 6-DOF non-linear rigid body dynamics, thrust and aerodynamic coefficients based on the MuPAL-α, and actuator models.

Fig. 1. JAXA's Multipurpose Aviation Laboratory (MuPAL-α) aircraft

A. Design results

The LPV model in (12), used for the development of the controller, is described in [10]. The scheduling parameter are

$$\rho = \begin{bmatrix} v_{ias} & v_{ias}^2 \end{bmatrix} \tag{42}$$

In this paper, the evaluation aims to verify the roll and sideslip tracking performance in the face of actuator faults. The lateral system states, selected to be those associated with the flight test described in [10], are roll angle ϕ, sideslip angle β, yaw rate r and roll rate p. The system inputs are differential trust δ_{td}, the aileron δ_a and rudder surface deflections δ_r. During the nonlinear simulations, differential trust and the rudder are assumed to be fault free. The command signals are the sideslip angle β_c and the roll angle ϕ_c. Knowledge of the control surface effectiveness levels, used in the control allocation component, are reconstructed from the adaptive sliding mode observer in Section II-A. During the simulation, the initial indicated airspeed is fixed around 120kts.

In the formulations, the discontinuous output injection signal v_l is approximated by

$$v_l = -k\frac{e_y}{|e_y|+\delta_l} \tag{43}$$

where the modulation gain $k = 40$ and the smoothing factor $\delta_l = 0.01$. To generate a smooth fault reconstruction signal, the learning rate τ in (10) is selected as 300. The initial value of $\hat{w}(0)$ is 1, which corresponds to a fault-free situation.

In the controller, a 'smooth' approximation of the discontinuous output injection signal

$$v_n = -\mathcal{K}(t,x)\frac{P_2 s(\rho)}{\|P_2 s(\rho)\|+\delta} \tag{44}$$

is used where the modulation gain $\mathcal{K} = 0.2$ and the smoothing factor $\delta = 0.05$. The selection of $M(\rho)$, the Lyapunov matrix P_2 and Φ are directly taken from [10]. From the LPV model, it is easy to estimate the upper bound of $\|B_2(\rho)\| = 10.7987$. The bound of the uncertainty error in fault estimate can be computed from Fig. 4 and it satisfies $\bar{\Delta} = 0.05$ for most of the time. Then from (41), the design parameter $\Delta_{max} = 1 - 0.5399/2.1731 = 0.7515$.

B. Simulation results

This section shows the nonlinear simulation results in a faulty situation. The trajectories of system states, in the faulty situation, are shown in Fig. 2. Clearly from Fig. 2, good roll and sideslip tracking performance is retained for the same manoeuvre despite the loss of 50% of the aileron effectiveness.

The reconstructed aileron effectiveness level, in the faulty situation, is shown in Fig. 3. Clearly from Fig. 3, the reconstructed aileron effectiveness level (blue line) converges to 0.5 (actual effectiveness level–red line) and therefore the loss of aileron effectiveness is well estimated. It is also clear from Fig. 3 that there exists small deviations just after 60sec due to the change of roll angle commands. Nevertheless, the fault estimate re-converges to 0.5. The (normalised) error in aileron fault estimation $\Delta(t)$ is shown in Fig. 4.

Fig. 5 show the smooth aileron and rudder demands and their surface deflection signals in the face of the 50% loss of aileron effectiveness. The sliding surfaces, associated with the sliding mode control law, are shown in Fig. 6 and it is clear that by choosing a suitable modulation gain and smoothing factor, the switching functions are maintained close to zero despite the change of roll angle commands.

IV. Fault reconstruction from flight test data

To further test the new FDI scheme proposed in this paper (prior to flight testing), earlier flight test data, collected from one of a series of actual flight tests conducted by a crew of JAXA personnel in January 2017 [10] will be used in an offline evaluation. Since the flight tests described in [10] only focused on evaluating the lateral-directional control performance, during the flight tests, longitudinal control of altitude and speed were manually maintained by the evaluation pilot through column and throttle lever inputs. The lateral-directional manoeuvres were created manually by the evaluation pilot via pedal and wheel manipulations which were translated into roll and sideslip commands. The lateral system states, inputs and reference commands are the same as those used for the nonlinear simulation. During the flight test, differential trust was not used for control allocation to mitigate risk. During the flight tests, a fault in the aileron was introduced giving a reduction in efficiency of 50%. For safety reasons, the fault was introduced at a software level. During the flight tests, air data inertial reference system (ADIRS) data and actuator performance levels were logged for monitoring and evaluation purposes [10].

The trajectories of the aircraft states associated with the lateral-directional motion are shown in Fig. 7. During the flight test, a coordinated 'S-turn' manoeuvre, with a roll angle of $\pm 20deg$ was introduced by the pilot. The actuator commands and their surface deflections are shown in Fig. 8. It can be seen from Fig. 8 that the fault free rudder operates at its full efficiency (the right figure in Fig. 8) and the aileron only operates at 50% efficiency due to the presence of the fault (the left figure in Fig. 8).

The fault reconstruction results from using the adaptive observer scheme proposed in this paper (in the face of a 50% aileron efficacy fault) are shown in Fig. 9. Clearly, the switching function is maintained close to zero. After sliding occurs, the fault reconstruction signal $\hat{w}$ (blue line) approximates the actual effectiveness of the actuator (red line) i.e. $w = 0.5$. It can also be seen from Fig. 9 that there exists a small deviation in the fault reconstruction signal just after 60sec. This is due to the steady turn manoeuvre in which the roll angle changes from 20 to -20 degree after 60sec (as shown in Fig. 7). A good estimate of the effectiveness level is achieved.

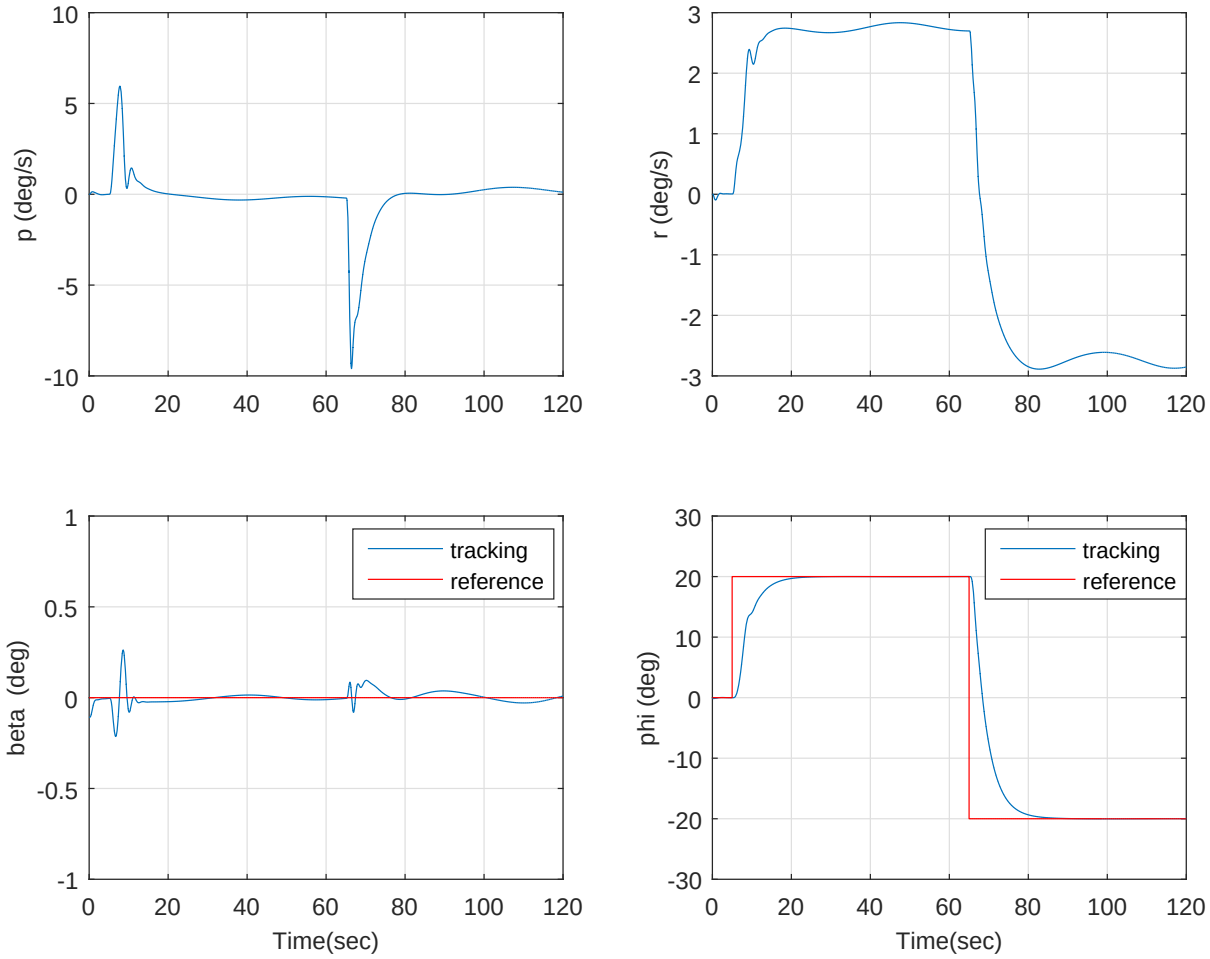

Fig. 2. The trajectories of states in the faulty situation

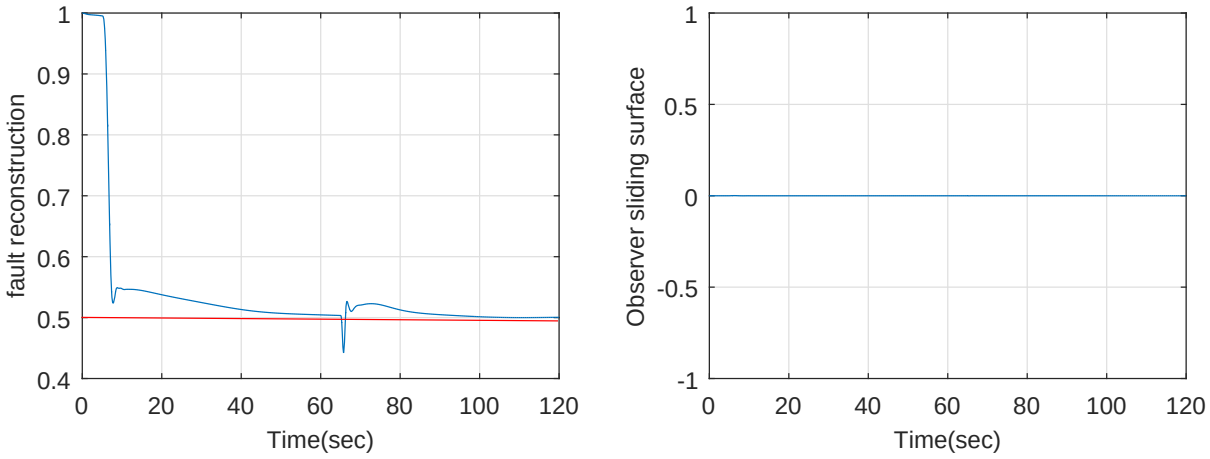

Fig. 3. Fault reconstruction performance in the faulty situation

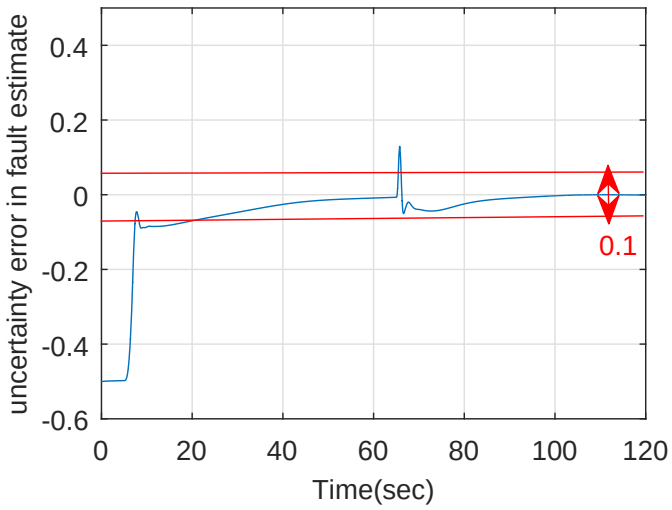

Fig. 4. The uncertainty error in aileron fault estimation

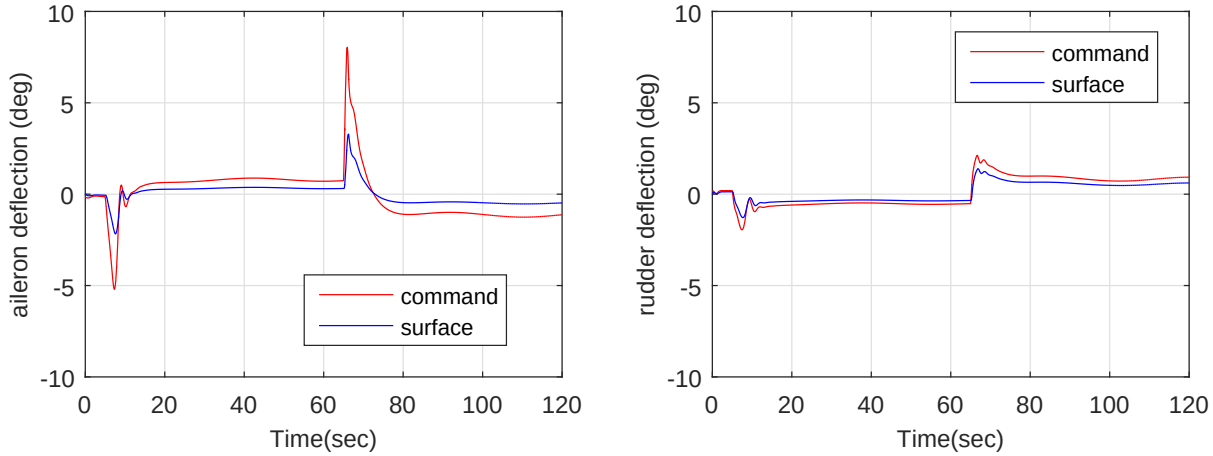

Fig. 5. Actuator deflections in the faulty situation

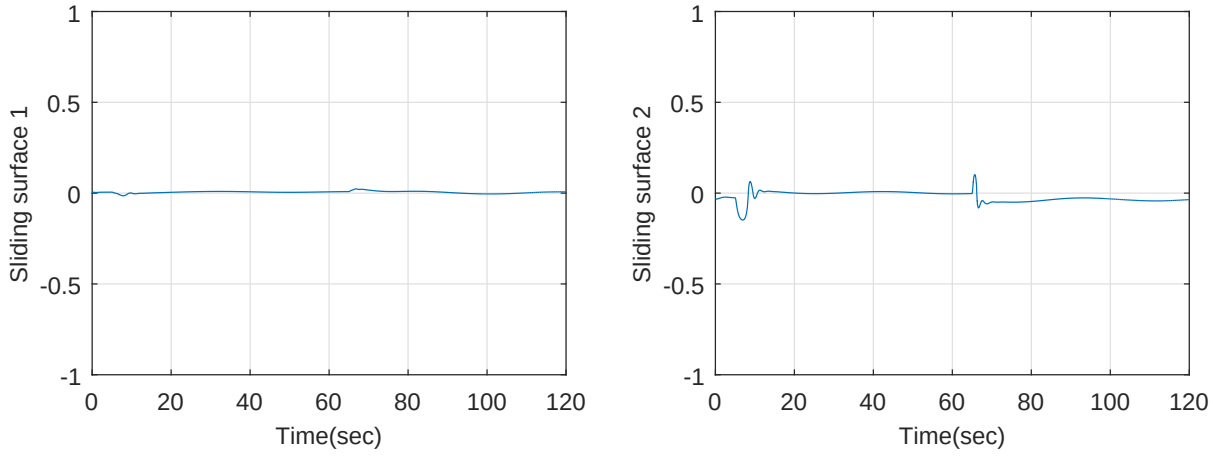

Fig. 6. Controller sliding surfaces in the faulty situation

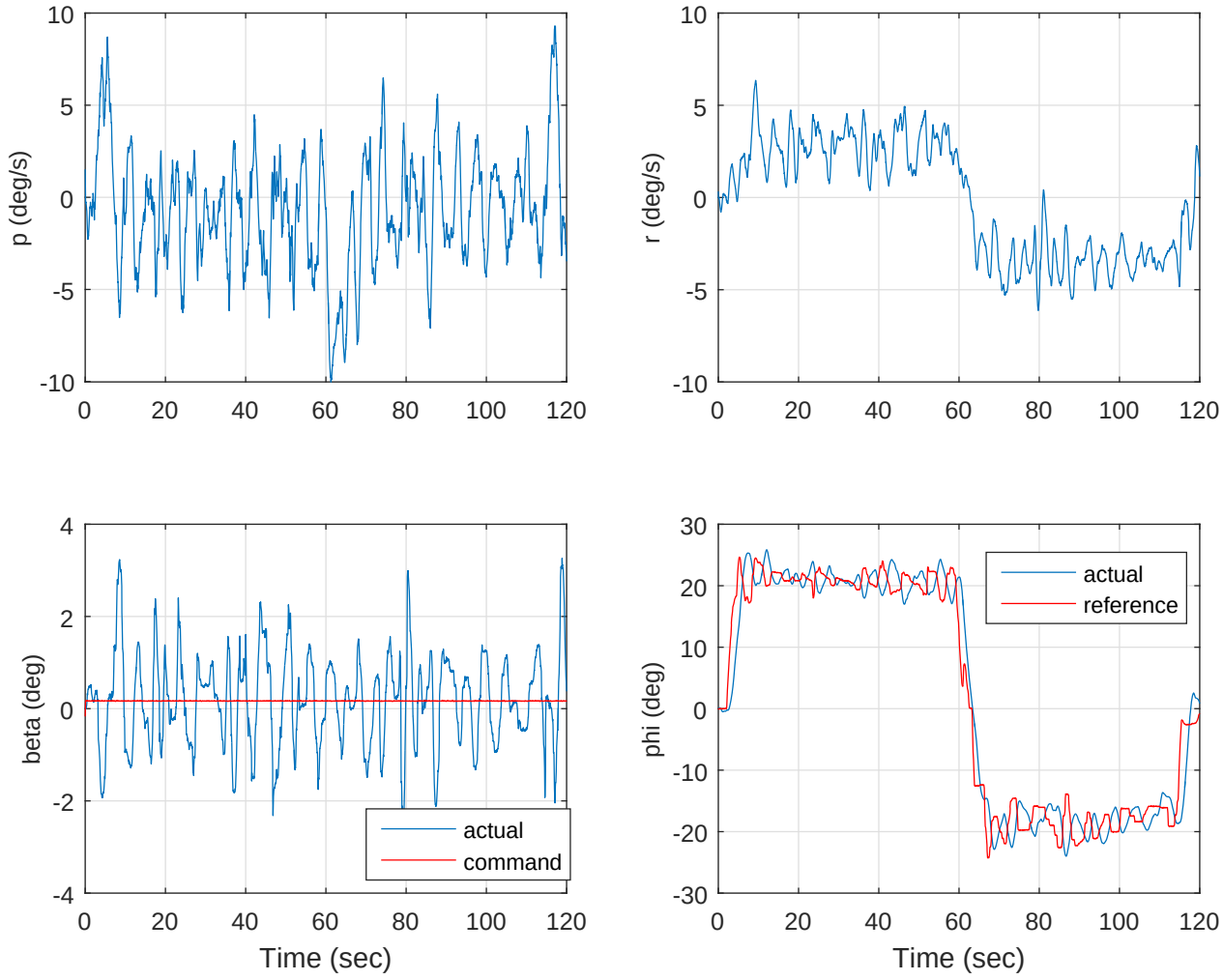

Fig. 7. States recorded during the flight test

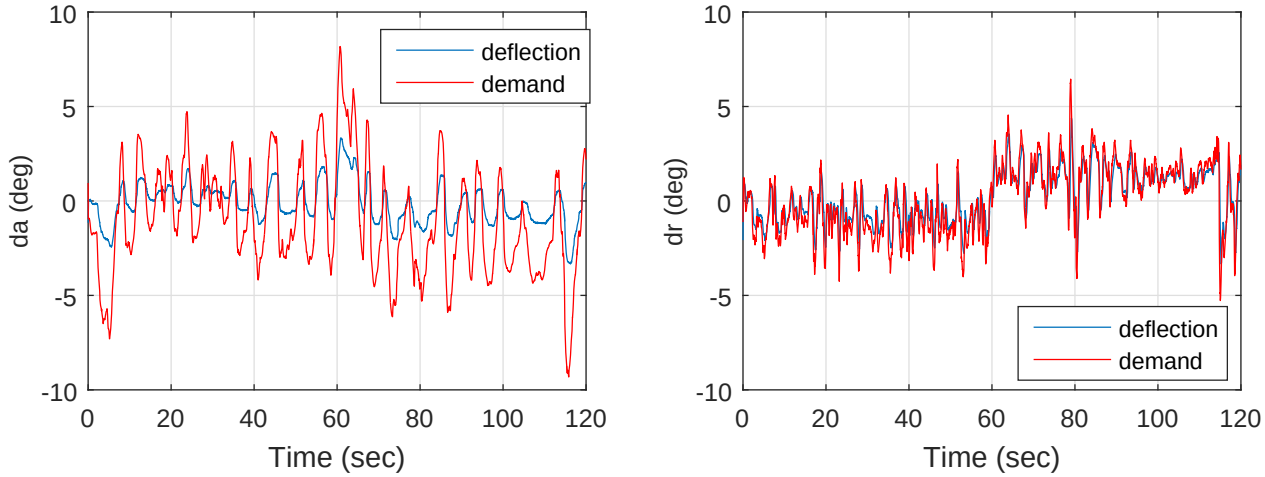

Fig. 8. Actuator demands and surface deflections

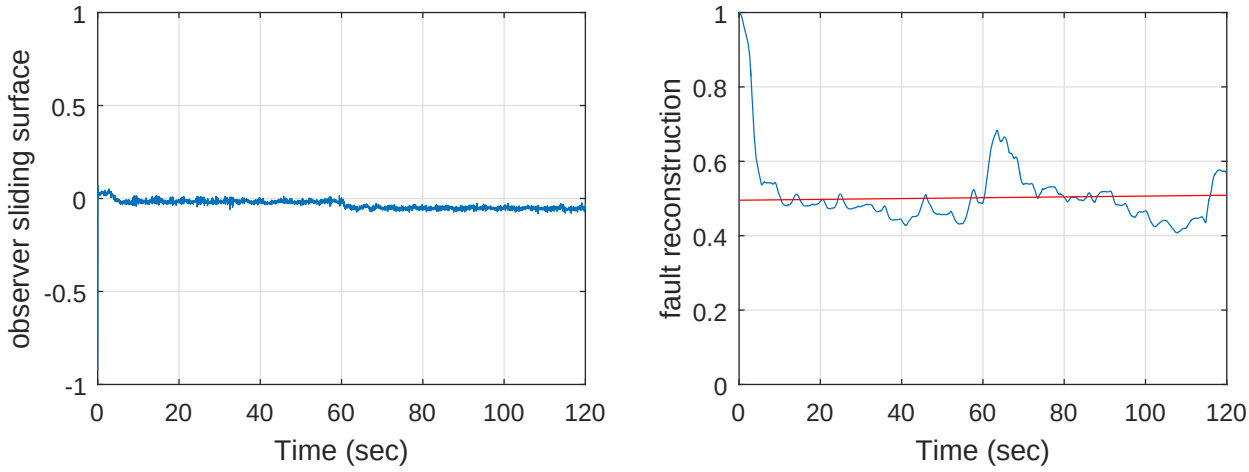

Fig. 9. Observer Sliding surface and Fault reconstruction

V. Conclusion

This paper has proposed an adaptive sliding mode observer to estimate the health levels of actuators at a 'local' level. Specifically the observer identifies the so-called effectiveness levels of each actuator. These effectiveness levels constitute an important component of an online control allocation based sliding mode scheme which can cope with a class of faults and total failures in overactuated systems. The proposed scheme was applied to the MuPAL-α nonlinear simulation model with the aileron only working at 50% effectiveness. The observer scheme has also been tested offline based on previously collected flight data from a previous MuPAL-α test flight in preparation for future flight test evaluations.

Acknowledgements

The authors appreciate the funding from the European Union Horizon 2020 research and innovation programme under grant agreement No. 690811 and the Japan New Energy and Industrial Technology Development Organization under grant agreement No. 062800, as a part of the EU/Japan joint research project entitled 'Validation of Integrated Safety-enhanced Intelligent flight cONtrol (VISION)'.

References

[1] C. Edwards, T. Lombaerts, and H. Smaili, *Fault tolerant flight control: A benchmark challenge*. Springer, 2010.
[2] P. Goupil and A. Marcos, "The European ADDSAFE project: Industrial and academic efforts towards advanced fault diagnosis," *Control Eng. Pract.*, vol. 31, pp. 109–125, 2014.
[3] P. Goupil, J. Boada-Bauxell, A. Marcos, P. Rosa, M. Kerr, and L. Dalbies, "An overview of the FP7 RECONFIGURE project: Industrial, scientific and technological objectives," in *SAFEPROCESS'15*, vol. 48, Pairs, France, 2015, pp. 976–981.
[4] P. Goupil, J. Boada-Bauxell, A. Marcos, E. Cortet, M. Kerr, and H. Costa, "AIRBUS efforts toward advanced real-time fault diagnosis and fault tolerant control," in *19th IFAC World Congress*, Cape Town, South Africa, 2014, pp. 3741–3746.
[5] V. Utkin, *Sliding modes in control and optimization*. Springer, 1992.
[6] H. Alwi, C. Edwards, and C. P. Tan, *Fault Detection and Fault-Tolerant Control Using Sliding Modes*. Springer, 2011.
[7] H. Alwi, C. Edwards, O. Stroosma, J. Mulder, and M. Hamayun, "Real-time implementation of an integral sliding mode fault tolerant control scheme for LPV plants," *IEEE Trans. Ind. Electron.*, vol. 62, pp. 3896–3905, 2015.
[8] M. T. Hamayun, C. Edwards, and H. Alwi, "A fault tolerant control allocation scheme with output integral sliding modes," *Automatica*, vol. 49(6), pp. 1830–1837, 2013.
[9] C. Edwards and S. K. Spurgeon, *Sliding Mode Control: Theory and Applications*. London, U.K.: Taylor & Francis, 1998.
[10] L. Chen, H. Alwi, C. Edwards, and M. Sato, "Flight evaluation of an LPV sliding mode controller with online control allocation," in *Proceedings of the IEEE CDC*, 2017, pp. 3928 – 3933.
[11] K. Masui and Y. Tsukano, "Development of a new in-flight simulator MuPAL-α," *AIAA paper 2000-4574*, Aug. 2000.
[12] M. Sato and A. Satoh, "Flight control experiment of multipurpose-aviation-laboratory-α in-flight simulator," *AIAA Journal of Guidance Control and Dynamics*, vol. 34, 2011.
[13] P. Goupil, "AIRBUS state of the art and practices on FDI and FTC in flight control system," *Control Eng. Pract.*, vol. 19, pp. 524 – 539, 2011.
[14] K. Zhang, B. Jiang, X.-G. Yan, and Z. Mao, "Adaptive robust fault-tolerant control for linear mimo systems with unmatched uncertainties," *Int. J. Control*, 2016.
[15] Q. Zhang, "Adaptive observer for multiple-input-multiple-output (MIMO) linear time-varying systems." *IEEE Trans. Autom. Control.*, vol. 47(3), pp. 525–529, 2002.
[16] D. Rotondo, F. Nejjari, V. Puig, and J. Blesa, "Model reference FTC for LPV systems using virtual actuator and set-membership fault estimation," *Int. J. Robust Nonlinear Control*, vol. 25, pp. 753–760, 2015.